PNAS
www.pnas.org

Supplementary Information for

Vertical Angular Momentum Constraint on Lunar Formation and Orbital History

ZhenLiang Tian and Jack Wisdom

Z. Tian, J. Wisdom
E-mail: zlt@ucsc.edu, wisdom@mit.edu

This PDF file includes:

Supporting Information Text

Model Comparison. Our model, which is the same as in (1), differs from the model of (2) in the following aspects:

1. Probably the most important difference is the tidal model. We use the conventional Darwin-Kaula constant Q model (3). In this model the tidal potential is expanded in a Fourier series and the response to each term is given a phase delay to model dissipation, by analogy to the damped harmonic oscillator. The explicit form builds in considerable constraints from orbital mechanics. There is little observational evidence to constrain the phase delays, but results from the analysis of lunar laser ranging (LLR) data are consistent with the Darwin-Kaula choice to set all the phase delays to be equal (4). Ćuk et al. (2) stated that there is a problem with the constant Q model: that it predicts a decay of orbital eccentricity that, to leading order, is independent of eccentricity. However, this is not true. Using the expressions in (3), one can show that the constant Q model gives a decay of eccentricity that is, to leading order, proportional to eccentricity. Nevertheless, given this misunderstanding of the constant Q model, Ćuk et al. proposed an ad hoc tidal model that introduced unjustified interpolation factors into the tidal model to fix a problem that does not exist. Tidal models used in long term simulations always represent a compromise between accuracy and computational efficiency. Another tidal model, the constant Δt model (5), is also commonly used for long-term studies, even though it is not supported by LLR results (4). Ideally, one would show that key model results are insensitive to the tidal model, as was done in (6), but this is not always a practical option. The rate of change of the eccentricity of the lunar orbit is a competition between an increase due to tides raised on the Earth and a decrease due to tides raised on the Moon. The constant Q model underestimates the observed rate of eccentricity increase, but there is a component of this increase that is not at present understood (4). Though imperfect, we feel that the best choice, at present, for long-term studies is the conventional constant Q tidal model.

2. We update the moment of inertia of the Earth (C_e), while (2) kept C_e as a constant throughout the evolution. The treatment of C_e affects the evolution of the rotation rate ω and J_2, and therefore the location of the Laplace plane transition.

   In its early history when the Earth was rotating fast, using the (7) scheme, C_e is much larger than the present value of $0.33 M_e R_e^2$ ($R_e = 6371$km). Assuming a two-layered structure, with core density $\rho_{core} = 12.35 \times 10^3 kg \cdot m^{-3}$, mantle density $\rho_{mantle} = 4.18 \times 10^3 kg \cdot m^{-3}$, with the present Earth core radius of 3483km, equatorial radius a_e of 6378km, polar radius of 6357km, the equatorial radius and polar moment of inertia for several rotation periods, T, are, according to Eq. 11-16 in (7):

$$\begin{aligned} T = 2.5h \quad &\rightarrow \quad a_e = 7659\text{km}, \quad C_e = 0.3353 M_e a_e^2 = 0.48 M_e R_e^2 \\ T = 3.0h \quad &\rightarrow \quad a_e = 7024\text{km}, \quad C_e = 0.3323 M_e a_e^2 = 0.40 M_e R_e^2 \\ T = 4.0h \quad &\rightarrow \quad a_e = 6675\text{km}, \quad C_e = 0.3318 M_e a_e^2 = 0.36 M_e R_e^2 \end{aligned}$$

   We update C_e by first updating J_2 (defined as $(C_e - A_e)/(M_e R_e^2)$) as $J_2^p(\omega/\omega^p)^2$, and then evaluating C_e and A_e by keeping $A_e + A_e + C_e$ equal to the present value. This is an oversimplified scheme, but it gives C_e values similar to (7).

3. We use the intrinsic wobble damping rate in (8) and (9) to damp the wobble of the Moon, while the rate of damping in (2) is 13 times smaller. Lunar laser ranging results are consistent with the (8) value (10). The damping time scale is

$$\tau = 3GC_m Q_m / (R_m^5 \omega_m^3 k_{2m}),$$

   where k_{2m} is the lunar Love number, Q_m is the Moon's tidal dissipation factor, R_m is the Moon's radius, ω_m is the Moon's rotation rate, and C_m is the Moon's moment of inertia.

4. We do not include the solar tides and the cross tides. According to (6), the changes due to these tides are minor (see Fig. 1).

Analytical Proof of the Conservation of L_z. The Hamiltonian of the Earth-Moon system without tides, when averaged over the lunar orbit and the Earth's orbit around the Sun, is

$$\begin{aligned} \mathscr{H}_{EM} = & C_1(1-e^2)^{-\frac{3}{2}}(\frac{3}{4}\cos^2\epsilon - \frac{1}{4}) \\ & + C_2(\frac{3}{4}\cos^2 I_e - \frac{1}{4}) \\ & + C_3[(\frac{3}{4}\cos^2 i - \frac{1}{4})(1+\frac{3}{2}e^2) + \frac{15}{8}\sin^2 i \cdot e^2 \cos 2\omega], \end{aligned} \quad [S1]$$

where the constant factors are

$$C_1 = -\frac{Gm_0 m_1}{a_1}\frac{J_2 R_e^2}{a_1^2}, \quad [S2]$$

$$C_2 = -\frac{Gm_0m_2}{a_2}\frac{J_2R_e^2}{a_2^2}, \quad [S3]$$

$$C_3 = -\frac{1}{2}\frac{Gm_rm_2}{a_2}\frac{a_1^2}{a_2^2}, \quad [S4]$$

and $m_0 = M_e$, m_1, m_2 are masses of the Earth, Moon, and Sun, $m_r = m_0m_1/(m_0 + m_1)$ is the reduced mass.

I_e is Earth's obliquity to the ecliptic, and $\cos I_e = H_0/G_0$.

l_0, g_0, h_0, L_0, G_0, H_0 are Andoyer coordinates and momenta for the Earth: G_0 is the spin angular momentum of the Earth (*i.e.*, $G_0 = L^{\oplus}$), L_0 is the component of the spin angular momentum on the symmetry axis of the Earth (for principal-axis rotation without wobble, $L_0 = G_0$), H_0 is the component of the spin angular momentum perpendicular to the ecliptic (*i.e.*, $H_0 = L^{\oplus}\cos I_e$). H_0 is conjugate to h_0, the longitude of the ascending node of the equator on the ecliptic (6).

a_1 is the semimajor axis of the lunar orbit (we will also denote it as a), e is the orbital eccentricity, and i is the inclination to the ecliptic. $\cos i = H_1/G_1$, $e^2 = 1 - (G_1/L_1)^2$.

l_1, g_1, h_1, L_1, G_1, H_1 are Delaunay coordinates and momenta for the lunar orbit: $L_1 = \sqrt{m_r\mu a}$, $G_1 = L_1\sqrt{1-e^2}$, where $\mu = Gm_0m_1$.The momentum L_1 is conjugate to the mean anomaly l_1 of the lunar orbit, G_1 is conjugate to the argument of pericenter $g_1 = \omega$ of the lunar orbit, and H_1 is conjugate to the longitude of the ascending node $h_1 = \Omega$ of the lunar orbit on the ecliptic. $G_1 = L^{☾}$, $H_1 = L^{☾}\cos i$.

ϵ is the mutual obliquity of the Earth's spin axis to the normal of the lunar orbit.

$$\cos\epsilon = \cos i\cos I_e + \sin i\sin I_e\cos(h_1 - h_0). \quad [S5]$$

a_2 is the semimajor axis of the Earth's orbit around the Sun.

The constants C_1, C_2, C_3 will change once tides are introduced.

Eq. S1 is derived by a method analogous to the derivation in (6). Eq. S1 reduces to the Hamiltonian in (6) up to constant terms if $e = 0$. We assume a circular orbit of the Earth around the Sun in the derivation. Note that C_1, C_2, C_3 are slightly different from the definitions in (6).

Since in $\mathscr{H}_{EM}$ there are only two combinations of angles, $h_1 - h_0$ and g_1 (*i.e.*, ω), to formally reduce the dimension of the problem, we make a canonical transform to new coordinates $g = \omega$ and $h = h_1 - h_0$. Using the F_2-type generating function

$$F_2 = l_0L + l_1L' + g_1G + g_0G' + (h_1 - h_0)H + h_0H' \quad [S6]$$

we find

$l = l_0$, $l' = l_1$, $g = g_1$, $g' = g_0$, $h = h_1 - h_0$, $h' = h_0$,

$L = L_0$, $L' = L_1$, $G = G_1$, $G' = G_0$, $H = H_1$, $H' = H_0 + H_1$.

The lower-case coordinates are conjugate to the corresponding upper-case momenta. Among the new coordinates (l, l', g, g', h, h'), only g and h appear in the Hamiltonian. So the averaged system has two degrees of freedom, or four dimensions in phase space: $\{g, h, G, H\}$. L, L', G', and H' are constants of $\mathscr{H}_{EM}$, since l, l', g', and h' do not appear in $\mathscr{H}_{EM}$. Note that in $\mathscr{H}_{EM}$ (Eq. S1), I_e, i, and e are functions of H and G:

$$\cos I_e = (H' - H)/G',\ \cos i = H/G,\ e = \sqrt{1 - (G/L')^2} \quad [S7]$$

and ϵ is a function of I_e, i, and h.

The averaged Hamiltonian governs the short-term evolution of the system. Tides only affect the long-term evolution and can be ignored in short-term analysis.

Note that $L_z = H'$, so the z-component of the angular momentum is conserved under $\mathscr{H}_{EM}$. Tides between the Earth and Moon preserve L_z. Therefore, without solar tides and perturbations from other planets of the solar system, L_z of the Earth-Moon system is a conserved quantity. We remind the reader that the derivation above is valid only when the Earth-Moon system is not in or near any resonance that involves the Sun, since the system can be averaged to the form of Eq. S1 only when there is no resonance involving λ_2, the longitude of the Sun. When the Earth-Moon system evolves through the evection resonance (a resonance between $\Omega + \omega$ and λ_2) or the evection-related limit cycle, substantial decrease in L_z can occur.

Low-e Phases of Evolution. Lunar eccentricity is excited in both the resonant processes (e.g. the evection limit cycle) and the non-resonant LPT-instability process. Here we examine implications of L_z conservation during those phases of the evolution when $e \approx 0$.

Since both kinds of AM-draining mechanisms require an eccentric orbit to operate, L_s is nearly conserved when $e \approx 0$. Since the L_z-changing resonant mechanisms require a non-zero eccentricity, L_z is also nearly conserved. Note that this is an approximation. L_s and L_z actually oscillate with small amplitudes, and their average values slowly decrease due to the solar tide.

During phases of low e and high i, tides on the Earth expands a ($\delta_a > 0$), and the obliquity tides on the Earth and Moon both damp i ($\delta_i < 0$, Eq. 1-6 in (2) supplementary material). Based on the near-conservation of L_s and L_z, we can analyze the change of I_e while a increases and i decreases.

Through tides on the Earth, AM is transferred from Earth's spin to the lunar orbit, *i.e.*, $L^{\oplus}$ decreases and $L^{☾}$ increases by approximately the same amount, δ_L ($L_s = L^{\oplus} + L^{☾}$ is nearly conserved). $\delta_L > 0$, since $\delta_a > 0$ and $L^{☾} \propto \sqrt{a}$ when $e \approx 0$. In

the same interval, i decreases: $\delta_i < 0$. Let δ_{Ie} denote the change in I_e. To conserve $L_z = L^{☾}\cos i + L^{⊕}\cos I_e$, we must have $(L^{☾} + \delta_L)\cos(i+\delta_i) + (L^{⊕} - \delta_L)\cos(I_e + \delta_{Ie}) = L^{☾}\cos i + L^{⊕}\cos I_e$,so

$L^{⊕}\sin I_e \sin\delta_{Ie} = (\cos I - \cos I_e)\delta_L - L^{☾}\sin i \sin\delta_i$.

Therefore, when $e \approx 0$, while a expands ($\delta_L > 0$) and i decreases ($\delta_i < 0$), I_e will also vary. If $I_e \geq i$, then I_e will increase ($\delta_{Ie} > 0$). If $I_e < i$, the behavior of I_e depends on the rates of di/dt and da/dt. Indeed, starting from post-impact states where $i = I_e$, before encountering the LPT, I_e always increases while the Earth and Moon tides increase a and decrease i (Fig. 2).

For the L_z-consistent high-obliquity simulations shown in Fig. 2, the cases that have gone through LPT-instabilities and have not ended with unbound orbit (the $\{61°, 0.7Lr\}$, $\{65°, 0.8Lr\}$ cases) both have their post-LPT $I_e(\sim 50°)$ larger than $i(\sim 35°)$, so the post-LPT, low-e evolution will not bring I_e down to I_e^p.

In our simulations of post-LPT evolution, we find that I_e typically increases by $\sim 5°$ from after LPT to the present. Therefore, the post-LPT I_e must be at most $\sim 20°$ to be compatible with the present $I_e^p = 23.4°$.

Oscillation of L_z. We can use standard Lie perturbation theory to estimate the magnitude of the variations of L_z (11). The original Hamiltonian of the system (*i.e.*, the Hamiltonian before averaging) is

$$\begin{aligned}
\mathscr{H}_{full} =& \mathscr{H}_0 + \mathscr{H}_1,\\
\mathscr{H}_0 =& -\frac{m_r\mu^2}{2L_1^2} + \frac{G_0^2 - L_0^2}{2A} + \frac{L_0^2}{2C},\\
\mathscr{H}_1 =& \frac{Gm_0m_1}{r_1'}\frac{J_2R_e^2}{r_1'^2}P_2(\hat{s}\cdot\hat{x}_1') + \frac{Gm_0m_2}{a_2}\frac{J_2R_e^2}{a_2^2}P_2(\hat{s}\cdot\hat{x}_2') - \frac{Gm_rm_2}{a_2}\frac{r_1'^2}{a_2^2}P_2(\hat{x}_1'\cdot\hat{x}_2')\\
=& -C_1(\frac{r_1'}{a_1})^{-3}P_2(\hat{s}\cdot\hat{x}_1') - C_2\cdot P_2(\hat{s}\cdot\hat{x}_2') + 2C_3(\frac{r_1'}{a_1})^2P_2(\hat{x}_1'\cdot\hat{x}_2'),
\end{aligned} \tag{S8}$$

where r_1' and $\hat{x}_1'$ are the magnitude and direction of the first Jacobi vector connecting the Earth to the Moon, r_2' and $\hat{x}_2'$ are the magnitude and direction of the second Jacobi vector from the center of mass of the Earth-Moon system to the Sun, and $\hat{s}$ is the direction of the spin axis of the Earth, $\hat{s} = (\sin I_e \sin h_0, -\sin I_e \cos h_0, \cos I_e)$. Since we have assumed the second orbit to be circular, there is $r_2' = a_2$ and $\hat{x}_2' = (\cos n_2 t, \sin n_2 t, 0)$, where n_2 is the mean motion of the second orbit.

To calculate the variations in $L_z = H_0 + H_1$ we divide $\mathscr{H}_1$ into two parts: an averaged part $\bar{\mathscr{H}_1}$ (*i.e.*, $\mathscr{H}_{EM}$), and an oscillating part $\tilde{\mathscr{H}_1}$, which is removed when we do the averaging. So

$$\mathscr{H} = \mathscr{H}_0 + \bar{\mathscr{H}_1} + \tilde{\mathscr{H}_1},$$

in which $\mathscr{H}_0$ is the unperturbed Hamiltonian and is dominant in magnitude, and $\bar{\mathscr{H}_1}$ and $\tilde{\mathscr{H}_1}$ are perturbations. We will look at the $\bar{\mathscr{H}_1}$ term, and the C_1, C_2, C_3 terms of $\tilde{\mathscr{H}_1}$ separately.

Since $L_z = H'$, and $\bar{\mathscr{H}_1}$ does not depend on h', L_z is conserved by $\bar{\mathscr{H}_1}$. In actual evolution of the system, L_z varies because the full Hamiltonian $\mathscr{H}$ depends on $h' = h_0$ through $\tilde{\mathscr{H}_1}$.

The main variation in L_z occurs because of perturbations from the Sun. So the C_1 term, which is the interaction between the Earth and Moon and does not involve the Sun, does not contribute to the variation in L_z.

For the C_2 and C_3 terms in $\tilde{\mathscr{H}_1}$, the routine of determining each term's contribution to the oscillation of L_z is:

1. For $\mathscr{H} = \mathscr{H}_0 + \mathscr{H}^*$, we perform a Lie transform that eliminates $\mathscr{H}^*$:

   $$\mathscr{H}' = e^{L_W}(\mathscr{H} + \mathscr{H}^*),$$

   where $L_W F = \{F, W\}$, L_W is the Lie derivative with respect to the generator W, and the curly brackets indicate the Poisson bracket. The condition that determines W is that the small term is eliminated. This is

   $$\{\mathscr{H}_0, W\} + \tilde{\mathscr{H}^*} = 0.$$

   Since both the C_2 and C_3 terms of $\tilde{\mathscr{H}_1}$ explicitly contain t (through $\hat{x}_2'$), we work in the extended phase space in which t is a coordinate, and add T, the momentum conjugate to time, to $\mathscr{H}_0$.

2. The variables also transform. We are interested in the variations of L_z. The transformed L_z is $e^{L_W}L_z$.

   $$L_z' = e^{L_W}L_z = L_z + \{L_z, W\} + ...$$

   So the variations in L_z are simply computed as $\{L_z, W\}$.

The C_2 term in $\tilde{\mathscr{H}_1}$ is

$$-C_2(3/4)\sin^2 I_e \cos 2(n_2 t - h_0).$$

The equation determining W then simplifies to (for the C_2 term)

$$\frac{\partial W}{\partial t} = -C_2(3/4)\sin^2 I_e \cos 2(n_2 t - h_0).$$

This can be integrated to

$$W = -C_2(3/4)\sin^2 I_e \sin 2(n_2 t - h_0)/(2n_2).$$

The consequent variation in $L_z = H_0 + H_1$ is then

$$\{H', W\} = -C_2(3/4)\sin^2 I_e \cos 2(n_2 t - h_0)/n_2.$$

So the magnitude of the variation of L_z due to the C_2 term is just $-C_2(3/4)\sin^2 I_e/n_2$ (note that C_2 is negative), and the peak to peak amplitude is twice this

$$-C_2(3/2)\sin^2 I_e/n_2. \tag{S9}$$

The C_3 term in $\tilde{\mathscr{H}_1}$ is more complicated. Averaged over the lunar orbit, it is

$$\begin{aligned} 2C_3[&(1+3/2e^2)(3/8)\sin^2 i \cos 2(n_2 t - h_1) \\ &+ (15/32)e^2(1-\cos i)^2 \cos(2(n_2 t - h_1) + 2\omega) \\ &+ (15/32)e^2(1+\cos i)^2 \cos(2(n_2 t - h_1) - 2\omega)] \end{aligned}$$

The corresponding W is

$$\begin{aligned} W = C_3[&(1+3/2e^2)(3/8)\sin^2 i \sin 2(n_2 t - h_1) \\ &+ (15/32)e^2(1-\cos i)^2 \sin(2(n_2 t - h_1) + 2\omega) \\ &+ (15/32)e^2(1+\cos i)^2 \sin(2(n_2 t - h_1) - 2\omega)]/n_2 \end{aligned}$$

The variation is L_z is

$$\begin{aligned} \{H_0 + H_1, W\} = 2C_3[&(1+3/2e^2)(3/8)\sin^2 i \cos 2(n_2 t - h_1) \\ &+ (15/32)e^2(1-\cos i)^2 \cos(2(n_2 t - h_1) + 2\omega) \\ &+ (15/32)e^2(1+\cos i)^2 \cos(2(n_2 t - h_1) - 2\omega)]/n_2. \end{aligned}$$

The three terms have different frequencies, so we can get the peak magnitude by adding the magnitudes of each term

$$-2C_3[(1+3/2e^2)(3/8)\sin^2 i + (15/16)e^2(1+\cos^2 i)]/n_2.$$

Collecting terms, $-C_3(3/4)[(1-e^2)\sin^2 i + 5e^2]/n_2$, and the peak to peak amplitude is twice this

$$-C_3(3/2)[(1-e^2)\sin^2 i + 5e^2]/n_2. \tag{S10}$$

The total peak to peak variation of L_z is the sum

$$\begin{aligned} &(3/2)\{-C_2 \sin^2 I_e - C_3[(1-e^2)\sin^2 i + 5e^2]\}/n_2 \\ =&[4.4673 \times 10^{-6}(\frac{a_1}{R_e})^2(\sin^2 i - e^2 \sin^2 i + 5e^2) + 7.837 \times 10^{-7}(\frac{\omega}{\omega^p})^2 \sin^2 I_e]L_r. \end{aligned} \tag{S11}$$

This prediction agrees well with the observed amplitude in the numerical simulations, as shown in Fig. S2.

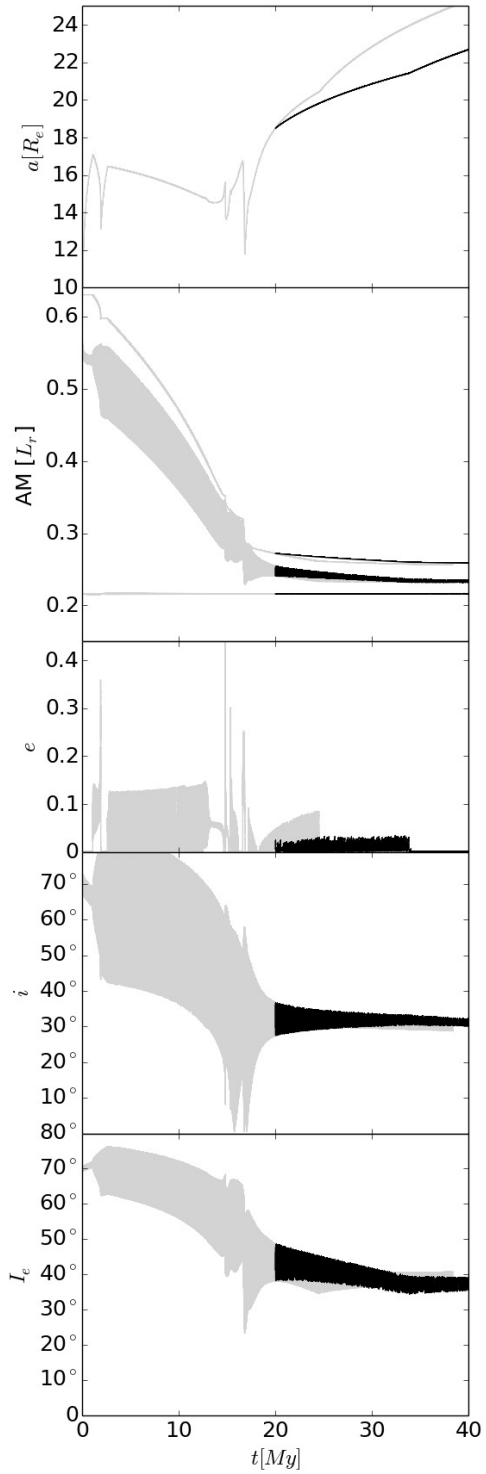

Fig. S1. Details of the Laplace transition, with the same choices of L_z-inconsistent initial conditions and parameters as for Fig. 1 in (2): $I_e = 70^\circ$, $L_s = 0.63L_r$, $Q_e/k_{2e} = 100$, $Q_m/k_{2m} = 100$. Black lines show a branching at 20 My with $Q_e/k_{2e} = 200$. In the AM panel, the top thin line is L_s (scalar sum, $L^\oplus + L^\leftmoon$), the thick band is $L^\oplus + L^\leftmoon \cos i$, and the horizontal thin line is L_z. This figure is to be compared to Fig. 1 in (2).

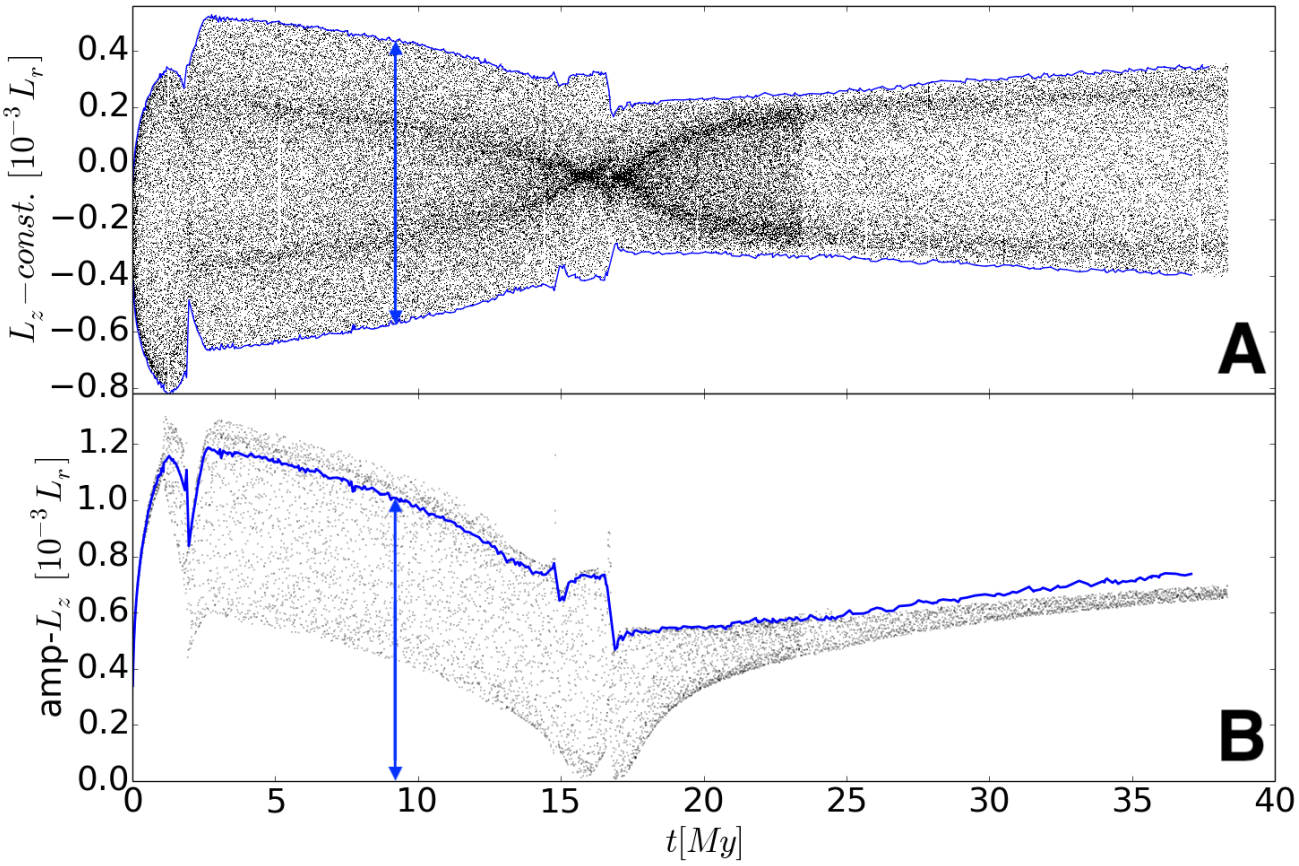

Fig. S2. (A) $L_z - 0.2162 L_r$ vs time, in $10^{-3} L_r$, for the same simulation in Fig. S1. (B) the predicted amplitude of L_z oscillation as suggested by Eq. S11. The blue lines in (A) are the envelopes of L_z data. The blue line in (B) shows the distance between the two envolopes in (A). The theoretical prediction agrees well with the measured amplitude as shown by the blue line.

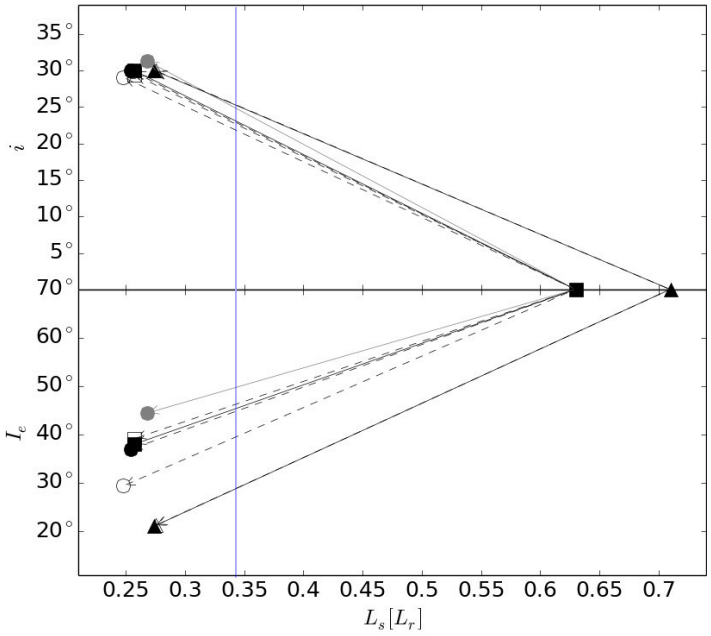

Fig. S3. L_s, i, and I_e results at $a = 25Re$, with the same choices of L_z-inconsistent initial conditions and parameters as for Fig. 2 in (2). Initial $I_e = 70^\circ$. Open square: $L_s = 0.63L_r$, $Q_e/k_{2e} = 100$, $Qm/k2m = 100$; black square is branching to $Q_e/k_{2e} = 200$ at 20 My. Circle: $L_s = 0.63L_r$, $Q_e/k_{2e} = 200$, $Qm/k2m = 200,\ 100,\ 50$ (white, grey, black). Open triangle: $L_s = 0.71L_r$, $Q_e/k_{2e} = 100$, $Qm/k2m = 100$; black triangle is branching to $Q_e/k_{2e} = 200$ at 28 My (left) and 30 My (right). Vertical blue line is $L_s = L_s^p$. All the cases end with L_s smaller than L_s^p. This figure is to be compared to Fig. 2 in (2).

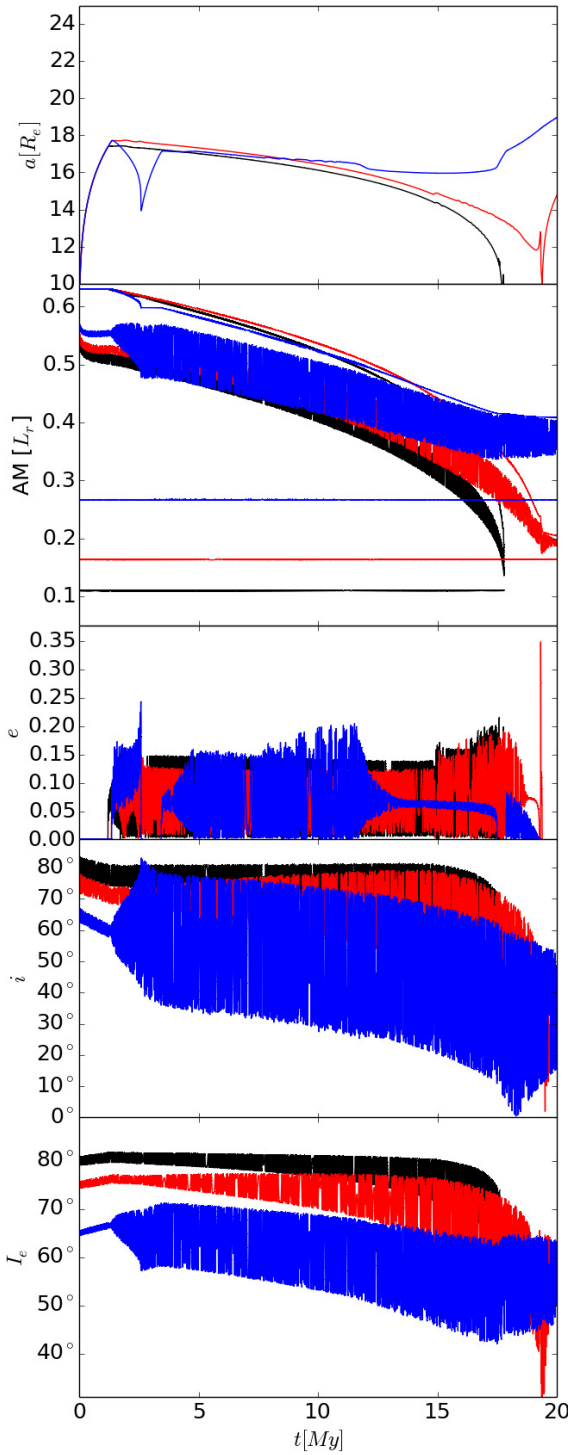

Fig. S4. Details of the Laplace transition, with the same choices of L_z-inconsistent initial conditions and parameters as for Fig. 3 in (2): $I_e = 80°$(black), $75°$(red), $65°$(blue), $L_s = 0.63L_r$, $Q_e/k_{2e} = 100$, $Q_m/k_{2m} = 100$. This figure is to be compared to Fig. 3 in (2).

Table S1. Vertical AM (L_z) used in (2) and our comparison simulations.

$L_z\,[L_r]$	L_z/L_z^p	$L_s\,[L_r]$	I_e	comment
0.215	63%	0.63	70°	Figs. S1, S3; Figs. 1, 2 in (2)
0.243	72%	0.71	70°	Fig. S3; Fig. 2 in (2)
0.109	32%	0.63	80°	Fig. S4; Fig. 3 in (2)
0.163	48%	0.63	75°	Fig. S4; Fig. 3 in (2)
0.266	78%	0.63	65°	Fig. S4; Fig. 3 in (2)

L_z^p is the present-day value of L_z $(0.339 L_r)$.

References

1. Wisdom J, Tian Z (2015) Early evolution of the Earth-Moon system with a fast-spinning Earth. *Icarus* 256:138–146.
2. Ćuk M, Hamilton DP, Lock SJ, Stewart ST (2016) Tidal evolution of the Moon from a high-obliquity, high-angular-momentum Earth. *Nature* 539(7629):402–406.
3. Kaula WM (1964) Tidal Dissipation by Solid Friction and the Resulting Orbital Evolution. *Rev. Geophys.* 2:661–685.
4. Williams JG, Boggs DH (2015) Tides on the Moon: Theory and determination of dissipation. *J. Geophy. Res. (Planets)* 120(4):689–724.
5. Mignard F (1979) The evolution of the lunar orbit revisited, I. *Moon Planets* 20:301–315.
6. Touma J, Wisdom J (1994) Evolution of the Earth-Moon system. *Astron. J.* 108:1943–1961.
7. Tricarico P (2014) Multi-layer Hydrostatic Equilibrium of Planets and Synchronous Moons: Theory and Application to Ceres and to Solar System Moons. *Astrophys. J.* 782:99.
8. Peale SJ (1973) Rotation of solid bodies in the solar system. *Reviews of Geophysics and Space Physics* 11:767–793.
9. Wisdom J, Meyer J (2016) Dynamic Elastic Tides. *Celestial Mechanics and Dynamical Astronomy* 126(1-3):1–30.
10. Williams JG, Boggs DH, Yoder CF, Ratcliff JT, Dickey JO (2001) Lunar rotational dissipation in solid body and molten core. *J. Geophy. Res. (Planets)* 106(E11):27933–27968.
11. Sussman GJ, Wisdom J (2015) *Structure and interpretation of classical mechanics, second edition.* (MIT Press).